NASA DEVELOP National Program
California – Ames

Fall 2024

San José Urban Development

Quantifying Canopy Cover and Land Surface Temperature in San José to Identify Future Tree Planting Sites

DEVELOP Technical Report
November 22nd, 2024

Shilpa Kannan, Analytical Mechanics Associates (Project Lead)
Patrick Kerwin, Analytical Mechanics Associates
Kathleen Miller, Analytical Mechanics Associates
Emeline Tu, Analytical Mechanics Associates

Advisors:
Dr. Morgan Gilmour, NASA Ames Research Center (Science Advisor)
Maya Hall, NASA Ames Research Center (Science Advisor)
Harrison Raine, NASA Ames Research Center (Science Advisor)
Lisa Tanh, Esri (Science Advisor)
Xihan Yao, Earth Define (Science Advisor)

Lead:
Lauren Webster (California – Ames)

1. Abstract

The urban heat island effect refers to the phenomenon of substantially increased temperatures in urban areas compared to their surrounding suburban or rural counterparts. The City of San José's Department of Parks, Recreation and Neighborhood Services (PRNS) and Department of Transportation (DOT) work to mitigate the UHI effect through urban forestry initiatives. The PRNS and DOT partnered with NASA DEVELOP to identify areas in need of tree plantings. We examined land surface temperature (LST) throughout the city using data from the Thermal Infrared Sensor (TIRS) and TIRS-2 on NASA's Landsat 8 and 9 satellites from 2013 to 2024. We also assessed canopy cover in parks using LiDAR data collected in 2020 for the United States Geological Survey's 3D Elevation Program, and measured vegetation greenness using the Normalized Difference Vegetation Index (NDVI) with PlanetScope imagery from 2018 to 2024. We evaluated social and environmental factors that influence the distribution of heat event impacts by creating a heat vulnerability index. We found that heat is concentrated in urban areas and that poor vegetation health is associated with high LST. We also found that socially vulnerable communities are disproportionately located in areas of high environmental risk. These analyses allow the partners to prioritize tree plantings in parks near areas of high social and environmental risk. We determined that Earth observations can be used to inform urban forestry decision making, but because methodologies for using LiDAR to assess canopy cover vary greatly, it is difficult to make comparisons across different canopy cover assessments.

Key Terms

land surface temperature, urban heat, NDVI, canopy cover, heat vulnerability, social vulnerability, Landsat, land cover change

2. Introduction

2.1 Background Information

The urban heat island (UHI) effect refers to the phenomenon of substantially increased temperatures in urban areas compared to their surrounding suburban or rural counterparts (Tamaskani Esfehankalateh et al., 2021). Causes of UHIs include restricted airflow between buildings, anthropogenic activity emissions, and absorption of solar radiation by impervious surfaces (Cheela et al., 2021; Tamaskani Esfehankalateh et al., 2021). With the increasing risk of extreme heat and rapid urbanization in cities across the globe, the effects of UHIs are a growing environmental and social concern (Tamaskani Esfehankalateh et al., 2021). The UHI effect can aggravate health effects of extreme heat, including heat stroke and heat-related mortality (Heidari et al., 2020). Moreover, studies have observed relationships between the severity of heat event impacts and sociodemographic vulnerability (Potter, 2021).

Past studies have shown that increasing vegetation cover through tree planting can reduce the effects of UHIs and lower urban land surface temperatures considerably (Loughner et al., 2012; Rogan et al., 2013). Tree canopies reduce ambient temperature by decreasing exposure to direct solar radiation through shade and by creating a cooling effect through evapotranspiration (Loughner et al., 2012). A comparative study on UHI mitigation strategies reported that increasing tree canopy cover in urban areas has been found to reduce ambient temperatures by up to 4° Celsius (7.2° Fahrenheit; Santamouris et al., 2017). Furthermore, studies examining social vulnerability to heat have found that tree canopy cover has a greater cooling effect in more socially vulnerable neighborhoods that lack trees, than in more affluent areas with higher levels of existing canopy and green spaces (Zhou et al., 2021).

To address these concerns, many urban heat studies have employed remote sensing technologies that help detect, map, and analyze the causes and impacts of UHIs. For instance, land surface temperature (LST), derived from remote sensing data, provides an indication of heat exposure and can be measured across a wide range of scales and locations (Hulley et al., 2019). In addition, measures of land cover and vegetation provide insight into the spatial characteristics that influence surface temperatures. For example, previous research has analyzed the relationship between LST and canopy cover using the Normalized Difference Vegetation Index (NDVI), which allows for the calculation and assessment of vegetation health (Grover & Singh, 2015). In

addition to vegetation health, measuring vegetation structure through Light Detection and Ranging (LiDAR) allows for accurate assessments of vegetation mass and provides more context by differentiating tree canopy from other vegetation (Elmes et al., 2017). Another valuable application of Earth observations and remote sensing analyses is through social and heat vulnerability assessments. Using remote sensing techniques and demographic census data, a recent study developed a Heat Vulnerability Index (HVI) to evaluate social and environmental factors that influence the distribution of heat event impacts (Qureshi & Rachid, 2022).

2.2 Study Area

San José, California (Figure 1) has a population of over one million and is located in Santa Clara County (U.S. Census Bureau, 2023). The county is known for its prominent technological innovation presence and has the third highest gross domestic product per capita in the world (Potter, 2021). Monitoring urban heat and canopy cover is important for understanding the distribution of UHI impacts in an area so densely populated and so important to the national and global economy. As heat waves become more frequent and more severe due to climate change, San José is looking to mitigate the harmful impacts of urban heat by fostering a healthy distribution of green spaces in the city (Romero, 2024).

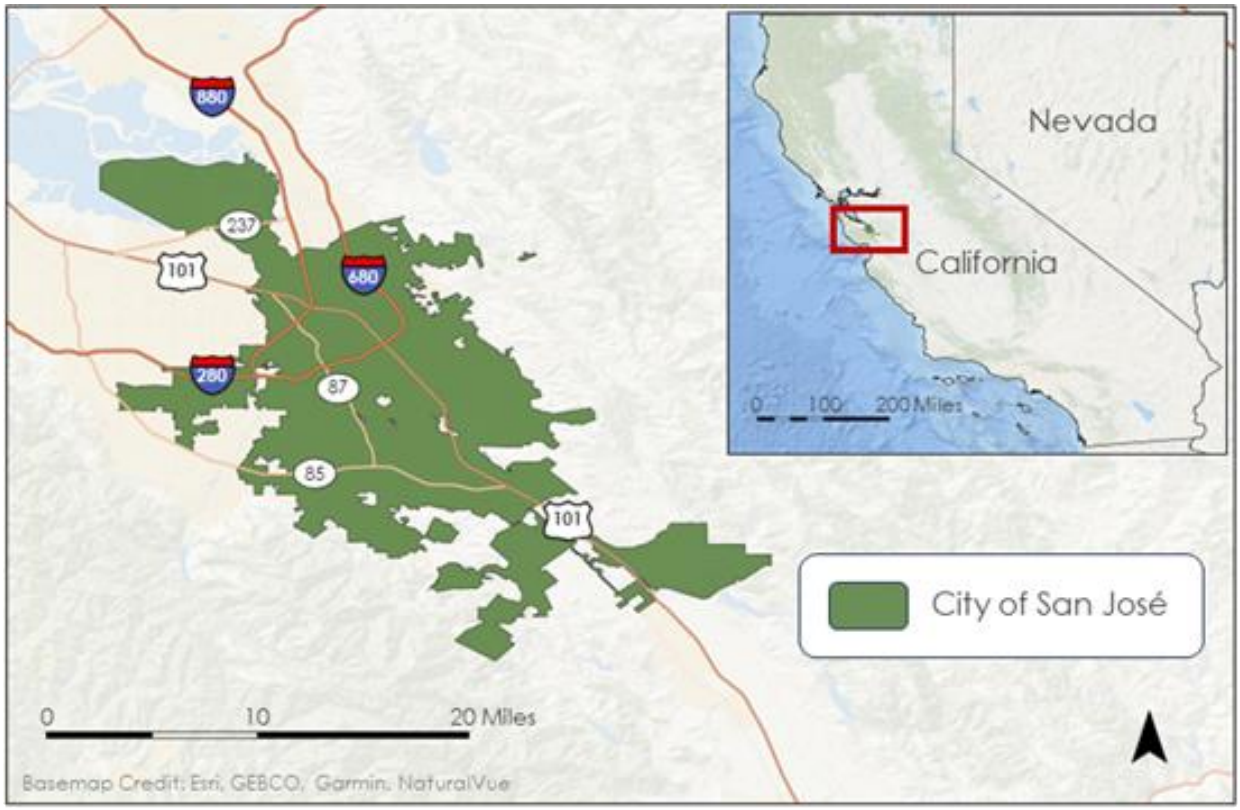

Figure 1. Study Area of San José, California

2.3 Project Partners and Objectives

Our team partnered with the City of San José's Department of Parks, Recreation and Neighborhood Services (PRNS) and Department of Transportation (DOT) to assess the feasibility of incorporating remote sensing techniques and NASA Earth observations into urban forestry initiatives to address community concerns about UHI impacts. The PRNS monitors and manages over 200 parks with a vision for "healthy communities that inspire belonging" (City of San José, n.d.a), and the DOT oversees city landscaping and supports community forestry (City of San José, n.d.b). The Community Forest Management Plan for the city reported a more than two square mile decrease in tree canopy cover between 2012 and 2018 and provides recommendations for how the PRNS and DOT may improve tree management (Dudek, 2022). To support the PRNS and DOT's forestry goals and inform decision making for future tree planting sites, this project

investigated the UHI effect in the study area of San José over a study period of 2013–2024. The team's primary objectives were to investigate LST, monitor changes in land cover, vegetation health, and tree canopy cover, and assess social vulnerability to heat in San José.

3. Methodology

3.1 Data Acquisition

3.1.1 Urban Heat

To investigate LST, we used Collection 2 Level 2 data from NASA's Landsat 8 Thermal Infrared Sensor (TIRS) and Landsat 9 TIRS-2. To collect the data, we accessed the PySTAC Planetary Computer Collection via the Python application programming interface using Python 3.12 in Visual Studio Code (Table 1). We developed a Python script to connect to this collection and select images that covered the study area from the years 2013–2024. To ensure clear images, we excluded images with more than 30% cloud cover or more than 5% null values.

Table 1
Datasets used in this study

Dataset	Spatial Resolution	Time Period	Description	Source
Landsat 8 TIRS	30m	2013–2021	Long-wave infrared band: used to calculate LST	PySTAC Planetary Computer
Landsat 9 TIRS-2	30m	2021–2024	Long-wave infrared band: used to calculate LST	PySTAC Planetary Computer
NLCD	30m	2013, 2016, 2019, 2021	Land cover classification: used to detect changes in land cover/land use	USGS National Land Cover Database
PlanetScope	3m	2018–2024	Red and near-infrared bands: used to calculate NDVI	Planet Explorer
Canopy Height Model	1m	2020	Canopy height: used to calculate canopy cover	Kabasares, K. (2024)
LiDAR Classification	1m	2020	LiDAR classification: used to calculate canopy cover	USGS
CDC/ATSDR SVI	N/A	2022	Social Vulnerability Index: used to create Heat Vulnerability Index	CDC ATSDR

3.1.2 Developed Land Cover

To understand the role that different land cover types play in the severity of UHI impacts, we acquired data from the United States Geological Survey (USGS) National Land Cover Database (NLCD) for the available individual years within our study period: 2013, 2016, 2019, and 2021. The database classifies land cover types into 16 different categories, including 4 different levels of developed land. We downloaded the data from the database, extracted the files, and imported them into ArcGIS Pro 3.3 for processing.

3.1.3 Vegetation

To assess changes in vegetation cover, we acquired PlanetScope imagery from Planet Explorer for the month of May in each year from 2018–2024. According to our partners, May is considered the growing period during which canopy cover is likely at its maximum level. We selected images that covered the entire study area and had cloud cover of less than 25% to ensure clear images. We then composited the selected images into a monthly view to use in our calculations.

3.1.4 Canopy Cover

To assess canopy cover across San José, we acquired a Canopy Height Model (CHM) and a LiDAR Classification that covered the entire study area. In 2020, Sanborn LLC captured the LiDAR data used for this CHM and classification under a contract with the USGS for the 3D Elevation Program. LiDAR is a remote sensing technology that uses laser pulses to measure the distance between the sensor and the Earth. This method captures differences in the height of a surface, such as San José's urban landscape, creating a digital surface model (DSM). When a digital terrain model showing differences in the elevation of the bare Earth is subtracted from the DSM, the outcome is the CHM. The CHM shows values for the height of anything that is taller than the bare Earth and trees, vegetation, and other built-up features such as buildings. When acquiring the CHM, we also received a classification layer that extracts and categorizes different types of features including vegetation and buildings. This provided us with the necessary data to estimate canopy cover in San José.

3.1.5 Heat Vulnerability

To construct a heat vulnerability index that assesses both social and environmental factors of heat risk, we began by creating a Social Vulnerability Index (SVI) for our study area. We collected data from the Centers for Disease Control and Prevention (CDC)/Agency for Toxic Substances and Disease Registry (ATSDR) SVI for the year 2022. This index includes metrics on socioeconomic status, household characteristics, racial and ethnic minority status, housing type, and transportation on a census tract level across California. We downloaded the data as a comma-separated values (csv) file from the CDC online data portal and uploaded it into R Studio v4.4 for further processing.

3.2 Data Processing

3.2.1 Urban Heat

To calculate LST, we selected the band lwir11 (long-wave infrared band) for further processing. We signed the URL of the long-wave infrared band using the odc.stac Python package to ensure that the data could be accurately retrieved. Once the bands were retrieved, we rescaled the raw temperature data to floating point values using the scale factor and offset. We then converted this from Kelvin to Fahrenheit. We aggregated the selected bands to create a median composite raster for the years 2013–2024 and 2018–2024. Using the rasterio package, we exported the median composite images as Tag Image File Format (TIFF) and imported the files into ArcGIS Pro for further processing.

3.2.2 Developed Land Cover

We used ArcGIS Pro to generate four preliminary land cover maps highlighting different levels of development for each year of data from 2018-2024. For each map, we clipped the land cover data to the boundaries of San José and added the census tract division lines as a layer on the map. We then filtered the land cover classifications for relevance, removing unnecessary classification types such as forest and shrubland types, and focused on various levels of developed areas to investigate any associations between urban development and LST. The levels of development from least to most developed based on the NLCD data legend were: Developed, Open Space; Developed, Low Intensity; Developed, Medium Intensity; and Developed, High Intensity.

3.2.3 Normalized Difference Vegetation Index

For each May composite PlanetScope image, we used the Raster Calculator tool in ArcGIS Pro to extract NDVI (Equation 1; Kriegler et al., 1969) values. To focus on the study area, we clipped the rasters to the San Jose city boundary. The output raster images had values ranging from -1 to 1 with -1 representing water, 0 representing barren land, and 1 representing healthy vegetation. To show vegetation greenness more clearly, we symbolized the maps with values from 0 to 1 to exclude non-vegetative surfaces such as buildings. Using ArcPy, we generated a median composite for the month of May from 2018 to 2024.

$$\text{NDVI} = \frac{(\text{NIR} - \text{Red})}{(\text{NIR} + \text{Red})} \quad (1)$$

3.2.4 Canopy Cover

We used the height values from the CHM and the vegetation information from the LiDAR classification to generate our canopy cover assessment. We used a conditional statement in ArcGIS Pro's Raster Calculator to create a new raster that only contained vegetation values with a height greater than two meters. This allowed us to isolate trees with canopy from other vegetation to use to estimate canopy cover. We then generated a polygon layer using the Raster to Polygon tool that shows canopy cover across the city.

3.2.5 Heat Vulnerability

To create the SVI component of our heat vulnerability assessment, we cleaned and filtered the data from the CDC/ATSDR SVI 2022 in R by limiting the county boundaries to Santa Clara County and removing unneeded metrics such as margin of error levels, population information, and area measurements. To assess for completeness, we used functions that checked for missing data, which ultimately confirmed that the dataset had no null values. We conducted an explorative data analysis in R through the tidyverse and DataExplorer packages to assess normalization and correlation levels of each category in the index. This helped us determine which variables were most influential in determining social vulnerability.

3.3 Data Analysis

3.3.1 Urban Heat

We imported TIFF files of the median LST data for the time spans of 2018–2024 and 2013–2024 into ArcGIS Pro to create two maps. First, we created a raster map that depicts median temperature distribution from 2018–2024 to compare against NDVI. We then used the Zonal Statistics tool to visualize the median temperatures in each census tract from 2013–2024 to compare against land cover change. We visually analyzed both maps to understand heat distribution throughout the study area. To assess the relationship between LST and NDVI, we used Microsoft Excel to analyze the difference in average temperature between census tracts with high NDVI and low NDVI values.

3.3.2 Developed Land Cover

To evaluate changes in the land cover of the study area within the study period, we employed the Change Detection Wizard in ArcGIS Pro to detect changes between the 2013 and 2021 map. We used the categorical change method to identify areas that had changed from any land cover category in 2013 to any level of developed land cover in 2021, including changes from developed land cover in 2013 to a different level of developed land cover in 2021. Next, we used the Raster to Polygon geoprocessing tool to convert all the developed areas in the change map to polygons for calculation. We then used the Summarize Within tool to determine the amount of area in square feet of each census tract that had experienced an increase in development from 2013 to 2021. Next, we converted the total area of each census tract into square feet. Finally, we calculated the percentage of area per census tract that experienced an increase in development to identify which census tracts had the most land developed over the 2013–2021 period.

3.3.3 Vegetation

We imported our TIFF file with the median NDVI for the month of May from 2018 to 2024. We used the Zonal Statistics tool to calculate the median NDVI value for each census tract in the city and used the Raster to Point tool to create a point at each pixel with the median NDVI value for each census tract. We then used the Summarize Within tool to isolate those values by census tract and join them to a polygon census tract layer for further analysis. We also generated a time-series animation showing how median NDVI in May changed in San José between 2018 and 2024 to visualize how vegetation has changed during the growing season for each year. We created this by using R to generate a Graphics Interchange Format (GIF) using maps exported from ArcGIS Pro with updated symbology made in Microsoft PowerPoint.

3.3.4 Canopy Cover

We validated the canopy cover output by visually comparing it with the tree inventory data from the San José open GIS portal and by comparing it with true color imagery. We used the canopy cover layer to calculate the

total canopy cover percentage in each park, census tract, and citywide using the Calculate Geometry and Calculate Field tools in ArcGIS Pro. This allowed us to get an overall citywide wide and park estimate. We also compared canopy cover with other environmental and social factors by census tract.

3.3.5 Heat Vulnerability

We normalized the data and performed a Principal Component Analysis in R to select five primary variable categories most significant in determining social vulnerability: 150% poverty, unemployment, housing cost burden, no high school diploma, and no health insurance. We used quantiles to score each census tract from 1-3 in each variable category, with 1 indicating the lowest impact of the variable category, and 3 the indicating highest impact of the variable category. We then summed all five categories to create an SVI with scores ranging from 5-15, with a score of 5-7 indicating low social vulnerability, and a score of 13-15 indicating high social vulnerability. We used ArcGIS Pro to map the SVI scores of each census tract.

To assess environmental factors of heat risk, we created an Environmental Risk Index (ERI), which incorporated data from the LST, canopy cover, and vegetation health assessments. We scored each census tract from 1-3 in each variable category for a total ERI score of 3-9, from low environmental risk to high environmental risk. A total score of 3 in the ERI indicated low LST, high canopy cover, and high vegetation health, while a score of 9 in the ERI indicated high LST, low canopy cover, and low vegetation health. We used ArcGIS Pro to map the ERI scores of each census tract.

To investigate the relationship between environmental risk factors and social vulnerability, we combined the ERI and SVI scores to create an HVI with a total range of 8-24. A score of 8 indicated the lowest level of heat vulnerability and a score of 24 indicated the highest level of heat vulnerability. We used ArcGIS Pro to create a bivariate map to visualize the HVI by census tract.

4. Results

4.1 Analysis of Results

4.1.1 Urban Heat

Figure 2 shows how the median temperature from 2018-2024 is distributed throughout the study area. Lower temperatures can be seen bordering the study area boundaries, such as the San Francisco Bay in the north or the Santa Cruz mountains in the South, while higher temperatures are more concentrated in the city center. Throughout the city, there is a clear contrast between the LST measurements of more highly developed areas and natural spaces such as parks and riparian zones. These areas show lower temperatures for both the immediate and surrounding areas. Our median LST census tract map depicts median temperature from 2013-2024 on a census tract level.

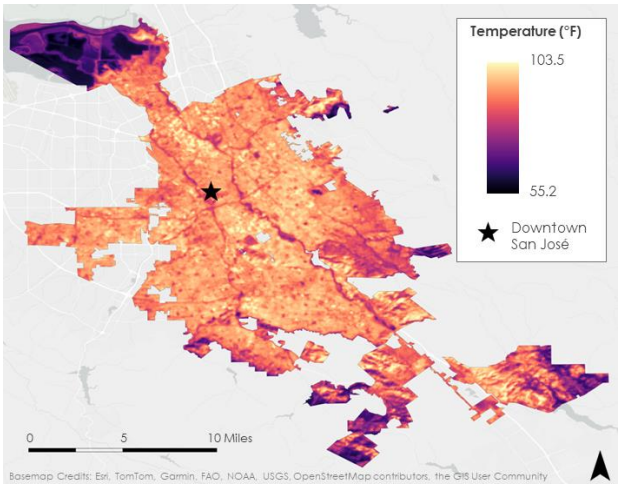

Figure 2. Median LST (°F) from 2018-2024 for San José.

4.1.2 Developed Land Cover

The NLCD land cover classification map shows all land cover types identified in San José in 2021 (Figure 3). This map provides context for the distribution of development in our study area and shows that most of the area in the city of San José is classified as Medium or High Intensity development. Figure 4 depicts the percentage of area per census tract that experienced an increase in development from 2013 to 2021. This includes areas that were undeveloped in 2013 that became developed by 2021. It also shows areas that were developed in 2013 that changed to a different level of development in 2021, such as from Developed, Open Space to Developed, High Intensity. The data showed that no areas classified as any level of Developed in 2013 decreased in development level by 2021. Therefore, any indication of change from the change detection analysis represented an increase in development level for that area. Moreover, areas classified as Developed, High Intensity in 2013 remained at that classification by 2021. Examples of increased development detected in the study area include large commercial areas with stores, restaurants, and parking lots, as well as those with an increased use of pavement and concrete in residential areas and parks.

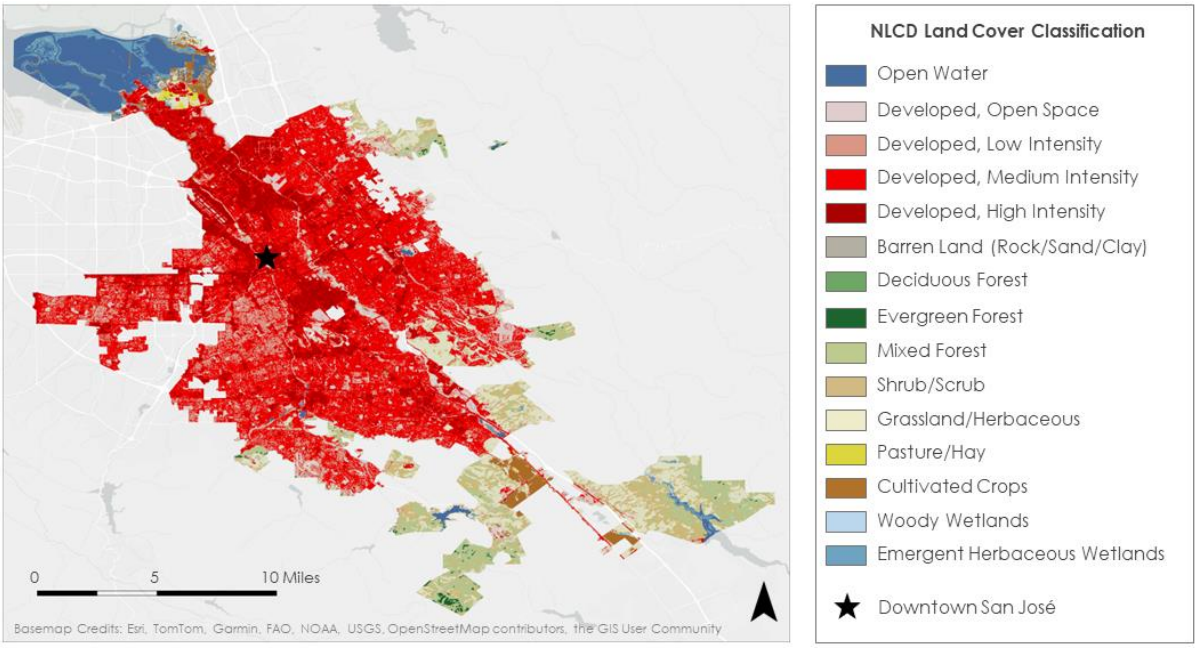

Figure 3. Land cover classification for San José in 2021

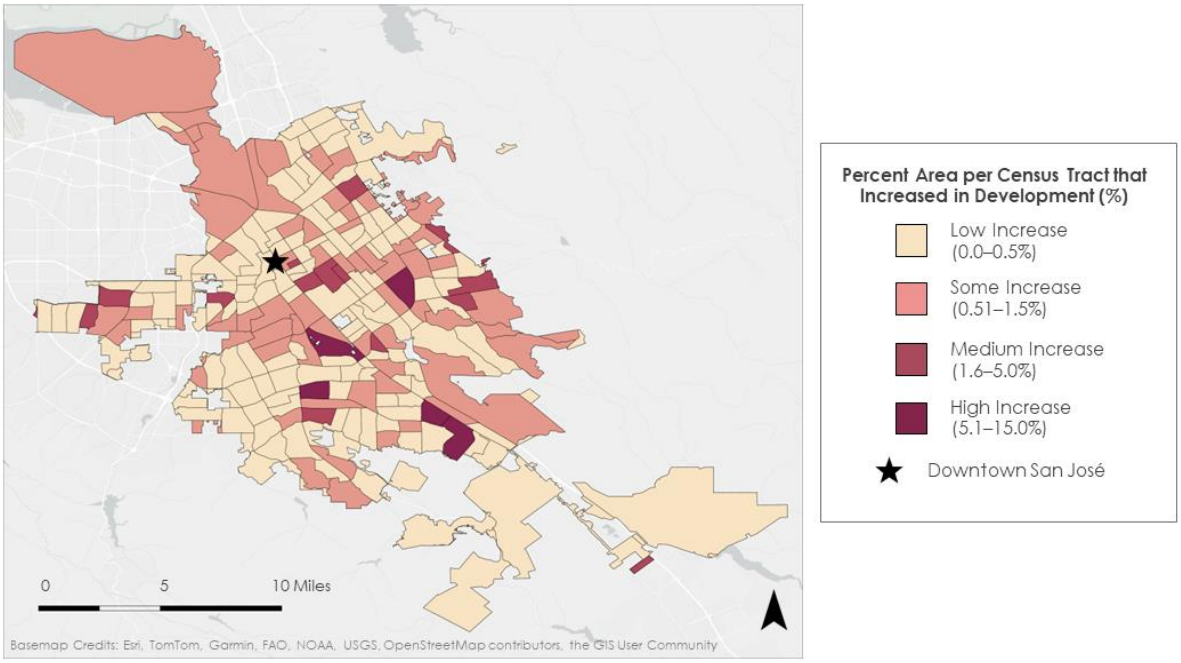

Figure 4. Percent of area per census tract that experienced an increase in development from 2013 to 2021 in San José (Landcover class: Developed, Open Space; Developed, Low Intensity; Developed, Medium Intensity; and Developed, High Intensity).

4.1.3 Vegetation

The median NDVI map for May 2018–2024 shows the distribution of vegetation throughout the city (Figure 5). Areas with healthy vegetation (or high vegetation greenness) are represented in dark green, while areas of low vegetation health or non-vegetative areas are indicated in yellow and light green. The data show concentrations of healthy vegetation near riparian areas and near bodies of water, as well as in parks. Census tracts on the western portion of the city and those that border mountainous, less-developed areas have a higher median NDVI (Figure 5). Census tracts closer to downtown and in the eastern portion of the city have lower median NDVI. When analyzing the relationship between urban heat and vegetation greenness, we found that these census tracts with a lower median NDVI had LST values that were on average 2°F higher than census tracts with a higher median NDVI.

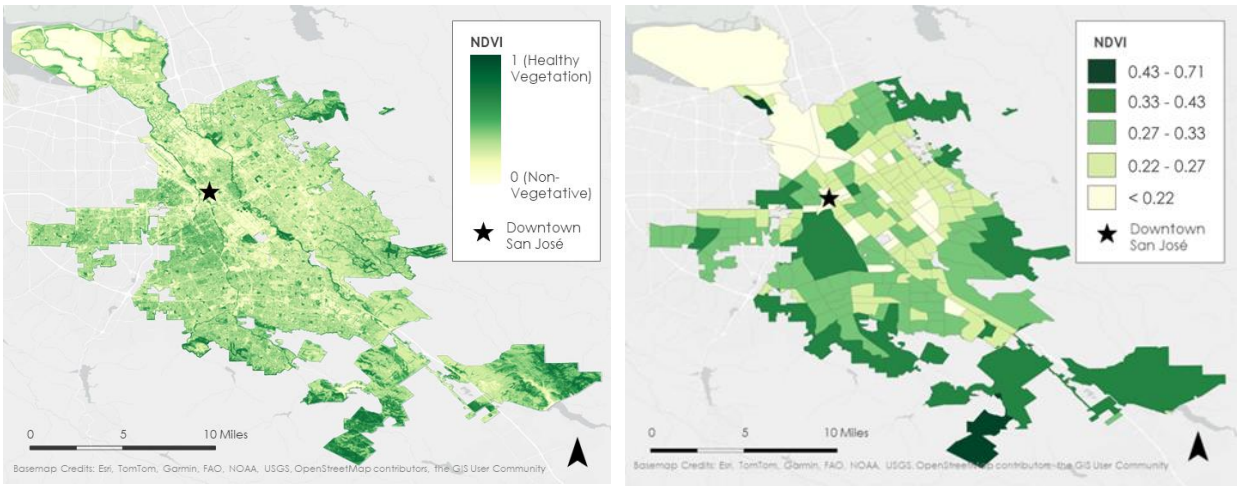

Figure 5. Median NDVI for the month of May 2018-2024 (left) and median NDVI by census tract (right) for the month of May 2018–2024 in San José. *Includes copyrighted material of Planet Labs PBC. All rights reserved.*

4.1.4 Canopy Cover

We found that canopy cover by census tract varied greatly across the city (Figure 6). Areas in the western portion of the city and along the edges had higher canopy cover than the eastern portion of the city. We calculated a city-wide canopy cover of 20.3%.

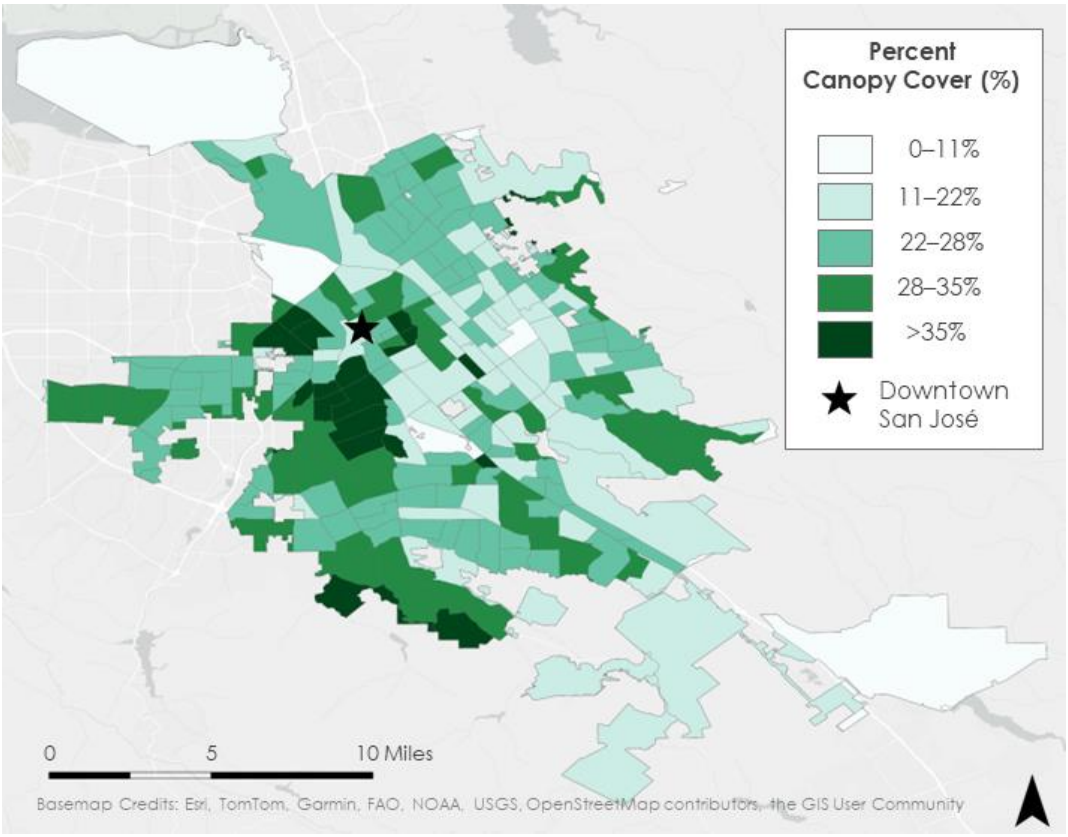

Figure 6. Canopy cover percentage by census tract in 2020 in San José.

4.1.5 Heat Vulnerability

The Heat Vulnerability Index bivariate map (Figure 7) shows associations between the Social Vulnerability Index (Figure A1) and Environmental Risk Index (Figure A2). When assessing the relationship between these two indices, we found that nearly 40% of census tracts with a high SVI score (13-15) are in areas of high environmental risk. In contrast, only 9% of census tracts with a low SVI score (5-7) are in areas of high environmental risk.

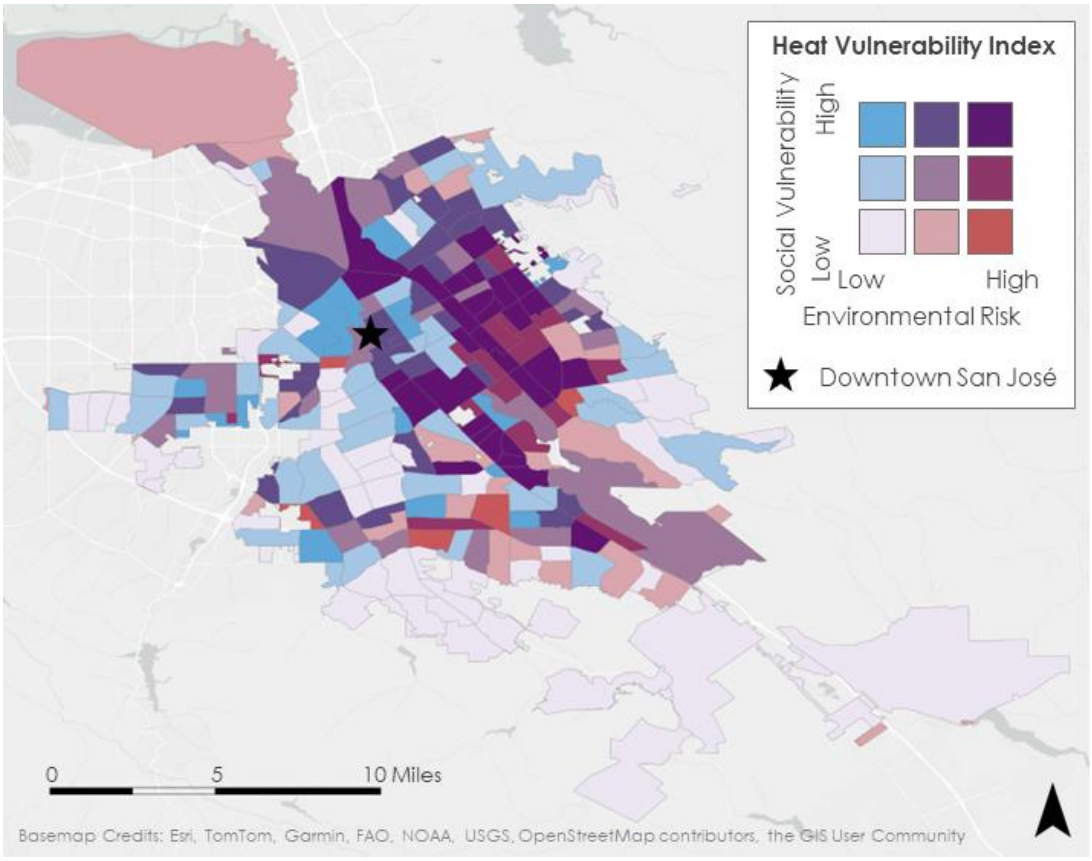

Figure 7. Heat Vulnerability Index

4.2 Errors & Uncertainties

The LST PySTAC script resulted in a varying number of images per year due to the presence of null values and cloud cover (Table B1). These images also varied by monthly distribution, with some years having at least one image per month and others missing images. This varying distribution can impact the median composite and bias the results as some months or years may be over or underrepresented. Furthermore, months with only one image can be impacted by outliers, as each image represents a singular day.

Originally, we hoped to use composite images from May and June for each year from 2018-2024 to calculate NDVI. Due to unreliable data for June during those years, we only used May for our calculations. This limitation may have affected our NDVI results because although the peak growing period tends to be in May in San José, it can vary slightly depending on precipitation and temperatures.

The canopy cover results indicate a slight over-estimation. Comparing with the City of San José's 2022 Community Forest Management Plan, we found that our results were slightly higher than their assessment city-wide. There are numerous methodologies for extracting vegetation from CHMs derived from LiDAR data which makes it difficult to compare across assessments.

5. Conclusions

5.1 Interpretation of Results

After analysis, we found that heat is concentrated in urban areas and were able to identify a spatial relationship between high intensity development areas and high LST. We also identified an association between high LST and low vegetation health. In census tracts with low vegetation greenness, LST temperatures were 2°F higher than in census tracts with high vegetation greenness. Our Heat Vulnerability

Index showed that socially vulnerable communities are disproportionately located in areas of high environmental risk. Finally, healthy vegetation levels in parks can reduce environmental risk in socially vulnerable areas.

5.2 Feasibility & Partner Implementation

We determined that it is feasible to use Earth observations to inform urban forestry decision making by visualizing and assessing environmental factors that influence urban heat. These insights will provide our partners additional resources to help them prioritize tree planting locations and maximize their impact in mitigating the effects of urban heat.

While LiDAR data can be used to assess canopy cover, differing methodology and data sources can make comparison difficult across canopy cover assessments. Although our canopy cover assessment will allow our partners to identify areas and parks with low canopy coverage, differences in methodology make it difficult for them to use our analysis to track canopy cover change versus their previous assessment. As the City of San José acquires more LiDAR data throughout the near and distant future, using one consistent method to calculate canopy cover from these data could allow them to compare between years.

6. Acknowledgements

We would like to thank the following people for their contributions to and support of our project:

Partners from the City of San José

- Kallie Schloemann – Department of Parks, Recreation and Neighborhood Services
- Nara Baker – Department of Transportation

Science Advisors

- Dr. Morgan Gilmour (NASA Ames Research Center)
- Maya Hall (California – Ames)
- Harrison Raine (NASA Ames Research Center)
- Lisa Tanh (Esri)
- Xihan Yao (EarthDefine)

DEVELOP Leads & Fellows

- Lauren Webster (California – Ames)
- Brent Bowler (Virginia – Langley)

Special Thanks

- Dr. Kyle Kabasares (NASA Ames Research Center)

This work utilized data made available through the NASA Commercial Smallsat Data Acquisition (CSDA) program.

This material is based upon work supported by NASA through contract 80LARC23FA024.

7. Glossary

ATSDR – Agency for Toxic Substances and Disease Registry; a United States government agency that addresses harmful health effects due to exposure to hazardous substances
CDC – Centers for Disease Control and Prevention; the national public health agency of the United States
CHM – Canopy Height Model; a raster layer that shows the height of trees, buildings, and other structures above the ground
Earth observations – Satellites and sensors that collect information about the Earth's physical, chemical, and biological systems over time
ERI – Environmental Risk Index; an index that uses environmental factors and spatial data to determine level of risk to an environmental hazard
HVI – Heat Vulnerability Index; an index that uses social vulnerability and environmental risk data to identify areas or populations most susceptible to heat risk
LST – Land Surface Temperature; the temperature of the surface of the Earth
Landsat 8 – an American Earth observation satellite developed in collaboration between the USGS and NASA, launched on February 11, 2013
Landsat 9 – an American Earth observation satellite developed in collaboration between the USGS and NASA, launched on September 27, 2021
LiDAR – Light Detection and Ranging; remote sensing technology that emits lasers to measure ranges (variable distances) to the Earth by detecting the time it takes the laser to return to the sensor
NLCD – National Land Cover Database; United States geospatial database created in collaboration between the USGS and the Multi-Resolution Land Characteristics (MRLC) Consortium
NDVI – Normalized Difference Vegetation Index; an index that measures vegetation health and density
PlanetScope – a European Space Agency (ESA) satellite constellation that provides remote sensing data for scientific research and application development
SVI – Social Vulnerability Index; an index that uses demographic data to determine the level of social vulnerability of a given area or population
TIRS – Thermal Infrared Sensor; a sensor on Landsat 8 (TIRS-2 on Landsat 9) that measures land surface temperature in two thermal infrared bands
UHI – Urban heat island; an urban area with substantially higher temperatures compared to surrounding suburban or rural areas, due to absorption of heat by impervious surfaces
USGS – United States Geological Survey; a United States government agency that leads science in the Department of the Interior and monitors, analyzes, and predicts Earth-system interactions

8. References

Centers for Disease Control and Prevention/ Agency for Toxic Substances and Disease Registry/ Geospatial Research, Analysis, and Services Program. CDC/ATSDR Social Vulnerability Index 2022 Database California. https://www.atsdr.cdc.gov/placeandhealth/svi/data_documentation_download.html

Cheela, V., John, M., Biswas, W., & Sarker, P. (2021). Combating Urban Heat Island Effect—A Review of Reflective Pavements and Tree Shading Strategies. *Buildings*, *11*(3), 93. https://doi.org/10.3390/buildings11030093ndvi

City of San José. (n.d.a). *ActivateSJ* [Government Website]. City of San José. https://www.sanjoseca.gov/your-government/departments-offices/parks-recreation-neighborhood-services/general-information/activatesj

City of San José. (n.d.b). *Landscaping* [Government Website]. City of San José. https://www.sanjoseca.gov/your-government/departments-offices/transportation/landscaping

Dudek. (2022). *San José Community Forest Management Plan.* https://www.sanjoseca.gov/home/showpublisheddocument/83642/637837331099770000

Earth Resources Observation and Science (EROS) Center. (2020). Landsat 8–9 Thermal Infrared Sensor Level–2, Collection 2 [dataset]. U.S. Geological Survey. https://doi.org/10.5066/P9OGBGM6

Elmes, A., Rogan, J., Williams, C., Ratick, S., Nowak, D., & Martin, D. (2017). Effects of urban tree canopy loss on land surface temperature magnitude and timing. *ISPRS Journal of Photogrammetry and Remote Sensing*, *128*, 338–353. https://doi.org/10.1016/j.isprsjprs.2017.04.011

Grover, A. & Singh, R. B. (2015). Analysis of Urban Heat Island (UHI) in Relation to Normalized Difference Vegetation Index (NDVI): A Comparative Study of Delhi and Mumbai. *Environments, 2*(2), 125–138. https://doi.org/10.3390/environments2020125

Heidari, H., Mohammadbeigi, A., Khazaei, S., Soltanzadeh, A., Asgarian, A., & Saghafipour, A. (2020). The effects of climatic and environmental factors on heat-related illnesses: A systematic review from 2000 to 2020. *Urban Climate*, *34*, 100720. https://doi.org/10.1016/j.uclim.2020.100720

Hulley, G., Shivers, S., Wetherley, E., & Cudd, R. (2019). New ECOSTRESS and MODIS Land Surface Temperature Data Reveal Fine-Scale Heat Vulnerability in Cities: A Case Study for Los Angeles County, California. *Remote Sensing*, *11*(18), 2136. https://doi.org/10.3390/rs11182136

Kabasares, K. (2024). Canopy Height Model derived from USGS 3DEP LiDAR data (CA SantaClaraCounty 2020). NASA Ames Research Center & Bay Area Environmental Research Institute. Data Processed from: U.S. Geological Survey, 2020, 3D Elevation Program Lidar Point Cloud (ver. CA SantaClaraCounty 2020).

Kriegler, F., Malila, W., Nalepka, R., & Richardson, W. (1969). Preprocessing transformations and their effect on multispectral recognition. Proceedings of the 6th International Symposium on Remote Sensing of Environment. Ann Arbor, MI: University of Michigan, 97-131.

Loughner, C. P., Allen, D. J., Zhang, D.-L., Pickering, K. E., Dickerson, R. R., & Landry, L. (2012). Roles of Urban Tree Canopy and Buildings in Urban Heat Island Effects: Parameterization and Preliminary Results. *Journal of Applied Meteorology and Climatology*, *51*(10), 1775–1793. https://doi.org/10.1175/JAMC-D-11-0228.1

Potter, C. (2021). Geography and Demographics of Extreme Urban Heat Events in Santa Clara County, California. *European Journal of Geosciences*, *3*(2), 1–10. https://doi.org/10.34154/2021-EJCC-0018/euraass

Qureshi, A. M., & Rachid, A. (2022). Heat Vulnerability Index Mapping: A Case Study of a Medium-Sized City (Amiens). *Climate*, *10*(8), 113. https://doi.org/10.3390/cli10080113

Rogan, J., Ziemer, M., Martin, D., Ratick, S., Cuba, N., & DeLauer, V. (2013). The impact of tree cover loss on land surface temperature: A case study of central Massachusetts using Landsat Thematic Mapper thermal data. *Applied Geography, 45*, 49–57. https://doi.org/10.1016/j.apgeog.2013.07.004

Romero, E. D. (2024, October 10). San José Just Had Its Hottest Week Ever, 'A Harbinger of Things to Come'. *KQED*. https://www.kqed.org/science/1994685/san-jose-just-had-its-hottest-week-ever-a-harbinger-of-things-to-come

Santamouris, M., Ding, L., Fiorito, F., Oldfield, P., Osmond, P., Paolini, R., Prasad, D., and Synnefa, A. (2017). Passive and active cooling for the outdoor built environment – Analysis and assessment of the cooling potential of mitigation technologies using performance data from 220 large scale projects. *Solar Energy, 154,* 14–33. https://doi.org/10.1016/j.solener.2016.12.006

Tamaskani Esfehankalateh, A., Ngarambe, J., & Yun, G. Y. (2021). Influence of Tree Canopy Coverage and Leaf Area Density on Urban Heat Island Mitigation. *Sustainability*, *13*(13), 7496. https://doi.org/10.3390/su13137496

United States Census Bureau. (2023). *City and Town Population Totals: 2020-2023* [Dataset]. https://www.census.gov/data/tables/time-series/demo/popest/2020s-total-cities-and-towns.html

U.S. Geological Survey, 2020, 3D Elevation Program Lidar Point Cloud (ver. CA SantaClaraCounty 2020), https://rockyweb.usgs.gov/vdelivery/Datasets/Staged/Elevation/LPC/Projects/CA_SantaClaraCounty_2020_A20/

U.S. Geological Survey, 2024, Annual NLCD Collection 1 Science Products: U.S. Geological Survey data release, https://doi.org/10.5066/P94UXNTS

Zhou, W., Huang, G., Pickett, S. T. A., Wang, J., Cadenasso, M. L., McPhearson, T., Grove, J. M., & Wang, J. (2021). Urban tree canopy has greater cooling effects in socially vulnerable communities in the US. *One Earth*, *4*(12), 1764–1775. https://doi.org/10.1016/j.oneear.2021.11.010

9. Appendices

Appendix A: *Environmental Risk Index and Social Vulnerability Index Maps*

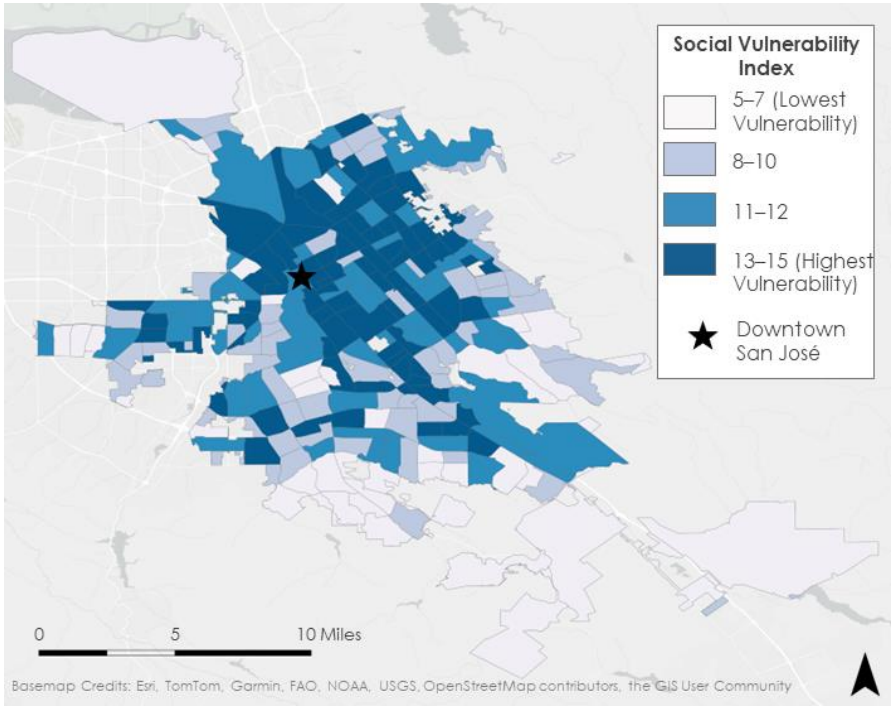

Figure A1. Social Vulnerability Index

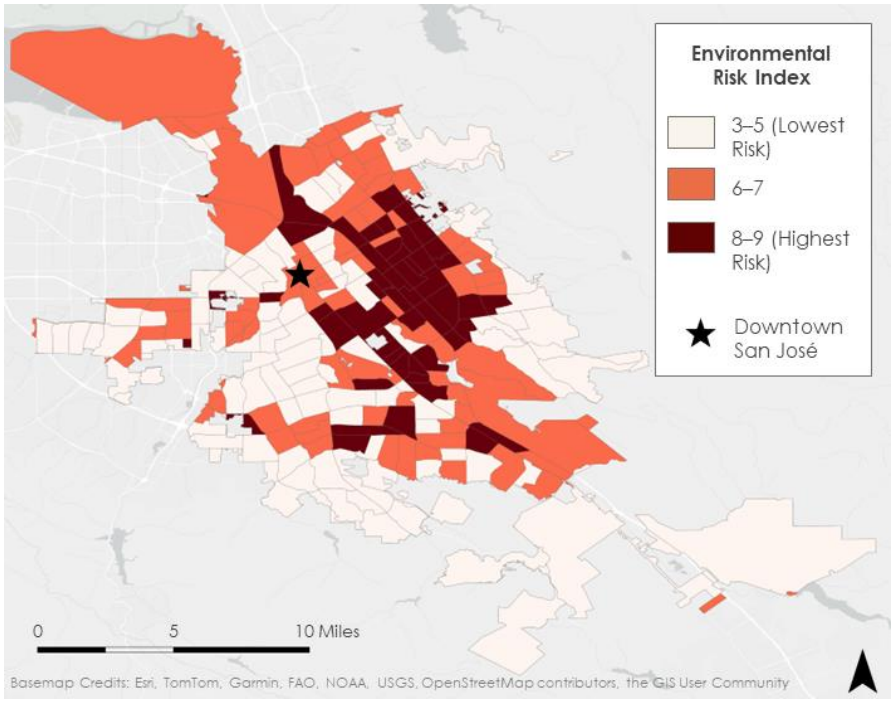

Figure A2. Environmental Risk Index

Appendix B: *Data Gaps for LST*

Table A1
Landsat 8 and Landsat 9 image availability per year

Year	**Total Images**	**Missing Months**
2013	8*	July
2014	11	February, June, August, November
2015	9	January, February, May, September, December
2016	11	January, May, July
2017	10	February, March
2018	8	January, May, July, September, December
2019	11	January, February, December
2020	12	January, August
2021	13	April, July
2022	22	September
2023	18	May, June, August
2024	8*	

*June-December 2013 and January-May 2024 were considered to ensure a full year view for the study period